

## Janus Scorpionates: Supramolecular Tectons for the Directed Assembly of Hard–Soft Alkali Metallopolymer Chains

Rosalice M. Silva,<sup>†</sup> Chengeto Gwengo,<sup>†</sup> Sergey V. Lindeman,<sup>†</sup> Mark D. Smith,<sup>‡</sup> and James R. Gardinier<sup>\*†</sup>

Department of Chemistry, Marquette University, Milwaukee, Wisconsin 53201-1881, and Department of Chemistry and Biochemistry, University of South Carolina, Columbia, South Carolina 29208

Received August 22, 2006

A new scorpionate ligand [HB(mtda)<sub>3</sub><sup>−</sup>] containing mercaptothiadiazolyl (mtda) heterocyclic rings with both hard nitrogen donors and soft sulfur donors has been prepared. This new ligand, the Janus scorpionate, is a hybrid of a tris(pyrazolyl)borate and a tris(mercaptoimidazolyl)borate. The differential hard/soft character of the dissimilar donor groups in this bridging ligand was exploited for the controlled solid-state organization of homometallic and heterometallic alkali metal coordination polymers. Remarkably, in the case of sodium, coordination polymers with both acentric (with NaS<sub>3</sub>N<sub>3</sub>H kernels) and centric (with alternating NaN<sub>6</sub> and NaS<sub>6</sub>H<sub>2</sub> kernels) chains are found in the same crystal (where the centricity is defined by the relative orientations of the B–H bonds of the ligands along the lattice). For the homometallic potassium congener, the larger cation size, compared to sodium, induced significant distortions and favored a polar arrangement of ligands in the resulting coordination polymer chain. An examination of the solid-state structure of the mixed alkali metal salt system revealed that synergistic binding of smaller sodium cations to the nitrogen portion and of the larger potassium cations to the sulfur portion of the ligand minimizes the ligand distortions relative to the homometallic coordination polymer counterparts, a design feature of the ligand that likely assists in thermodynamically driving the self-assembly of the heterometallic chains. The effect of alkali metal complexation on the solution properties of the ligand was studied by comparing NMR chemical shifts, B–H stretching frequencies, and electrochemical properties with those of the noncoordinating tetrabutylammonium salt of the scorpionate. The similarity of these data regardless of cation indicates that the salts are likely dissociated in solution rather than maintaining their solid-state polymeric structures. This data is augmented by the ESI(±) mass spectral data for a series of mixed alkali metal tris(mercaptothiadiazolyl)borates that also indicate that dissociation occurs in solution.

### Introduction

One area of contemporary research interest is the deliberate construction of molecular edifices using designed building blocks, or tectons, to control solid-state architectures<sup>1</sup> and possibly to also include desired functionality into a given

material.<sup>2</sup> Recently, there has been a resurgent interest in modification of the frameworks of the ubiquitous scorpionate ligands based on poly(pyrazolyl)borates and poly(pyrazolyl)methanes, first prepared by Trofimenko in the mid 1960s,<sup>3</sup> to give potentially multinucleating organic derivatives or metal complexes thereof (“metalloligands”) that can be incorporated into coordination networks.<sup>4,6–12</sup> For this reason,

\* To whom correspondence should be addressed. E-mail: james.gardinier@marquette.edu.

<sup>†</sup> Marquette University.

<sup>‡</sup> University of South Carolina.

- (1) (a) Hosseini, M. W. *Acc. Chem. Res.* **2005**, *38*, 313. (b) Hosseini, M. W. *CrystEngComm* **2004**, *6*, 318. (c) James, S. L. *Chem. Soc. Rev.* **2003**, *32*, 276. (d) Moulton, B.; Zaworotko, M. J. *Chem. Rev.* **2001**, *101*, 1629. (e) Robson, R. J. *Chem. Soc., Dalton Trans.* **2000**, 3735. (f) Blake, A. J.; Champness, N. R.; Hubberstey, P.; Li, W.-S.; Withersby, M. A.; Schröder, M. *Coord. Chem. Rev.* **1999**, *183*, 117. (g) Hagrman, P. J.; Hagrman, D.; Zubieta, J. *Angew. Chem., Int. Ed.* **1999**, *38*, 2638.

- (2) Janiak, C. *Dalton Trans.* **2003**, 2781.

- (3) (a) Trofimenko, S. *J. Am. Chem. Soc.* **1966**, *88*, 1842. (b) Trofimenko, S. *Scorpionates: The Coordination Chemistry of Polypyrazolylborate Ligands*; Imperial College Press: London, 1999.

- (4) For other recent coordination polymers based on metalloligands, see: (a) Noro, S.-I.; Miyasaka, H.; Kitagawa, S.; Wada, T.; Okubo, T.; Yamashita, M.; Mitani, T. *Inorg. Chem.* **2005**, *44*, 133. (b) He, Z.; He, C.; Gao, E.-Q.; Wang, Z.-M.; Yang, X.-F.; Liao, C.-S.; Yan, C.-H. *Inorg. Chem.* **2003**, *42*, 2206.

the syntheses of “third-generation” scorpionates (scorpionates modified at the fourth group bound to boron or on the methine carbon of the charge neutral counterpart)<sup>5</sup> have been pursued vigorously, and notable examples include the potentially ditopic ferrocenyl-linked poly(pyrazolyl)borates  $\{\text{Fe}[\text{C}_5\text{H}_4\text{B}(\text{pz})_3]_2\}^{2-}$ ,<sup>6a-c</sup>  $\{\text{Fe}[\text{C}_5\text{H}_4\text{B}(\text{Me})(\text{pz})_2]_2\}^{2-}$ ,<sup>6b-d</sup> the arene-linked poly(pyrazolyl)borates  $\{\text{C}_6\text{H}_4[\text{B}(\text{pz})_3]_2\}^{2-}$ ,<sup>6e</sup>  $\{\text{C}_6\text{H}_4[\text{B}(\text{tBu})(\text{pz})_2]_2\}^{2-}$ ,<sup>6e,f</sup> their charge neutral poly(pyrazolyl)methane analogues,  $[\text{C}_6\text{H}_{6-x}(\text{CH}_2\text{OCH}_2\text{C}(\text{pz})_3)_x]$  ( $x = 2, 3, 4, 6$ ),<sup>7</sup>  $\text{C}_6\text{H}_4[\text{CH}(\text{pz})_2]_x$  ( $x = 2, 3$ ),<sup>7e,f</sup>  $\text{Fe}[\text{C}_5\text{H}_4\text{CH}_2\text{OCH}_2\text{C}(\text{pz})_3]_2$ ,<sup>8a</sup>  $\text{Fe}[\text{C}_5\text{H}_4\text{CH}(\text{pz})_2]_2$ ,<sup>8b,c</sup> the alkane-linked derivatives  $(\text{CH}_2)_n[\text{CH}(\text{pz})_2]_2$  ( $n = 1-3$ ),<sup>8d,e</sup> and the first mixed tris(pyrazolyl)borate/tris(pyrazolyl)methane complexes,  $\text{Fe}[(\text{pz})_3\text{CCH}_2\text{OCH}_2\text{C}_2\text{C}_6\text{H}_4\text{B}(\kappa^3\text{-N}, \text{N}', \text{N}''\text{-pz})_3]_2$  and  $\text{Fe}\{3,5\text{-}[(\text{pz})_3\text{CCH}_2\text{OCH}_2]_2\text{C}_6\text{H}_3\text{C}_2\}\text{C}_6\text{H}_4\text{B}(\kappa^3\text{-N}, \text{N}', \text{N}''\text{-pz})_3\}^{2-}$ .<sup>9</sup> Somewhat overlooked for the purpose of constructing supramolecular assemblies based on scorpionate building blocks is the modification of the pyrazolyl rings either with additional coordinating moieties such as cyano groups<sup>10</sup> and *meta*- or *para*-pyridyls,<sup>11</sup> or even modifying the pyrazolyl

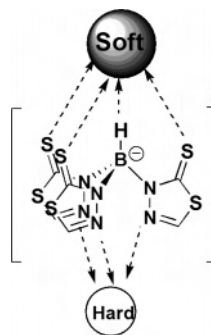


Figure 1. Potential coordination behavior of Janus scorpionates.

ring system itself by replacing the CHs with donor atoms as in the case of the poly(1,2,4-triazolyl)borates.<sup>12</sup>

Our interest in the coordination and supramolecular chemistry of potentially multinucleating scorpionate ligands composed of electroactive, sulfur-containing, *N*-heterocyclic ligands<sup>13</sup> prompted us to consider scorpionates based on mercaptothiadiazolyls, as in Figure 1. The choice of mercaptothiadiazolyls was inspired in part by the potential for the different donors to induce a controlled organization of metallochains according to Pearson’s hard–soft acid–base concept.<sup>14</sup> The choice of mercaptothiadiazolyls was also encouraged by the important electrochemical activity of this group and related heterocycles (exploited in battery applications),<sup>15</sup> and the potentially desirable surface adsorption properties of this ring system<sup>16</sup> that may allow for layer-by-layer self-assembly of future conducting materials. The ligand design in Figure 1 represents a hybrid of Trofimenko’s first generation tris(pyrazolyl)borates and of Reglinski’s tris(mercaptoimidazolyl)borates,<sup>17</sup> and close relatives of Bailey’s

- (5) First-generation scorpionates generally refer to the simple  $[\text{HB}(\text{pzR})_3]^-$  ligands. Second-generation scorpionates, also invented by Trofimenko, are those with bulky groups at the 3-position of the pyrazolyl, see: Trofimenko, S.; Calabrese, J. C.; Thompson, J. S. *Inorg. Chem.* **1987**, *28*, 1507.
- (6) (a) Fabrizi de Biani, F.; Jaekle, F.; Spiegler, M.; Wagner, M.; Zanello, P. *Inorg. Chem.* **1997**, *36* (10), 2103. (b) Herdtweck, E.; Jaekle, F.; Opromolla, G.; Spiegler, M.; Wagner, M.; Zanello, P. *Organometallics* **1996**, *15* (26), 5524. (c) Jaekle, F.; Polborn, K.; Wagner, M. *Chem. Ber.* **1996**, *129* (6), 603. (d) Ilkhechi, A. H.; Bolte, M.; Lerner, H.-W.; Wagner, M. *J. Organomet. Chem.* **2005**, *690* (8), 1971. (e) Bieller, S.; Zhang, F.; Bolte, M.; Bats, J. W.; Lerner, H.-W.; Wagner, M. *Organometallics* **2004**, *23* (9), 2107. (f) Zhang, F.; Bolte, M.; Lerner, H.-W.; Wagner, M. *Organometallics* **2004**, *23* (21), 5075.
- (7) (a) Reger, D. L.; Semeniuc, R. F.; Rassolov, V.; Smith, M. D. *Inorg. Chem.* **2004**, *43*, 537. (b) Reger, D. L.; Semeniuc, R. F.; Smith, M. D. *Inorg. Chem.* **2003**, *42*, 8137. (c) Reger, D. L.; Semeniuc, R. F.; Silaghi-Dumitrescu, I.; Smith, M. D. *Inorg. Chem.* **2003**, *42*, 3751. (d) Reger, D. L.; Brown, K. J.; Gardinier, J. R.; Smith, M. D. *J. Organomet. Chem.* **2003**, *666*, 87. (e) Reger, D. L.; Brown, K. J.; Smith, M. D. *J. Organomet. Chem.* **2002**, *658*, 50. (f) Reger, D. L.; Semeniuc, R. F.; Smith, M. D. *Inorg. Chem.* **2001**, *40*, 6545. (g) Reger, D. L.; Wright, T. D.; Semeniuc, R. F.; Grattan, T. C.; Smith, M. D. *Inorg. Chem.* **2001**, *40*, 6212. (h) Reger, D. L.; Watson, R. P.; Smith, M. D.; Pellechia, P. J. *Organometallics* **2006**, *25*, 743. (i) Reger, D. L.; Watson, R. P.; Smith, M. D.; Pellechia, P. J. *Organometallics* **2005**, *24*, 1544.
- (8) (a) Reger, D. L.; Brown, K. J.; Gardinier, J. R.; Smith, M. D. *J. Chem. Crystallogr.* **2005**, *35*, 221. (b) Reger, D. L.; Brown, K. J.; Gardinier, J. R.; Smith, M. D. *J. Organomet. Chem.* **2005**, *690*, 1889. (c) Reger, D. L.; Brown, K. J.; Gardinier, J. R.; Smith, M. D. *Organometallics* **2003**, *22*, 4983. (d) Reger, D. L.; Watson, R. P.; Gardinier, J. R.; Smith, M. D. *Inorg. Chem.* **2004**, *43*, 6609. (e) Reger, D. L.; Gardinier, J. R.; Semeniuc, R. F.; Smith, M. D. *J. Chem. Soc., Dalton Trans.* **2003**, 1712.
- (9) Reger, D. L.; Gardinier, J. R.; Bakbak, S.; Bunz, U. W. E.; Smith, M. D. *New J. Chem.* **2005**, *8*, 1035.
- (10) (a) Siemer, C. J.; VanStipdonk, M. J.; Kahol, P. K.; Eichhorn, D. M. *Polyhedron* **2004**, *23*, 235. (b) Rheingold, A. L.; Incarvito, C. D.; Trofimenko, S. *Inorg. Chem.* **2000**, *39*, 5569.
- (11) Pyrazolyl groups with the hydrogen at the 3-position replaced with *ortho*-pyridyls (or 2-pyridyls) tend to give chelate complexes rather than coordination polymers and can be considered second-generation. Those with the 3-position of pyrazolyl substituted with *para*- or *meta*-pyridyls on the other hand give multimetallic compounds, see: (a) Adams, H.; Batten, S. R.; Davies, G. M.; Duriska, M. B.; Jeffery, J. C.; Jensen, P.; Lu, J.; Motson, G. R.; Coles, S. J.; Hursthouse, M. B.; Ward, M. D. *Dalton Trans.* **2005**, *11*, 1910. (b) Davies, G. M.; Jeffery, J. C.; Ward, M. D. *New J. Chem.* **2003**, *27*, 1550. (c) Weis, K.; Vahrenkamp, H. *Inorg. Chem.* **1997**, *36*, 5589.
- (12) Janiak, C.; Scharmann, T. G.; Albrecht, P.; Marlow, F.; Macdonald, R. *J. Am. Chem. Soc.* **1996**, *118*, 6307.
- (13) (a) Silva, R. M.; Liddle, B. J.; Lindeman, S. J.; Smith, M. D.; Gardinier, J. R. *Inorg. Chem.* **2006**, *45*, 6794. (b) Silva, R. M.; Smith, M. D.; Gardinier, J. R. *Inorg. Chem.* **2006**, *45*, 2132. (c) Silva, R. M.; Smith, M. D.; Gardinier, J. R. *J. Org. Chem.* **2005**, *70*, 8755.
- (14) (a) Pearson, R. G. *J. Am. Chem. Soc.* **1963**, *85*, 3533. (b) Pearson, R. G., Ed. *Hard and Soft Acids and Bases*; Dowden, Hutchinson & Ross: Stroudsburg, PA, 1973. (c) For examples, exploiting the same methodology, see: Baudron, S. A.; Hosseini, M. W. *Inorg. Chem.* **2006**, *45*, 5260. (d) Humphrey, S. M.; Mole, R. A.; McPartlin, M.; McInnes, E. J. L.; Wood, P. T. *Inorg. Chem.* **2005**, *44*, 5981. (e) Jouaiti, A.; Hosseini, M. W.; Cian, A. D. *Chem. Commun.* **2000**, 1863. (f) Krautscheid, H.; Emig, N.; Klaassen, N.; Senger, P. *J. Chem. Soc., Dalton Trans.* **1998**, 3071.
- (15) (a) Tannai, H.; Tsuge, K.; Sasaki, Y.; Hatozaki, O.; Oyama, N. *Dalton Trans.* **2003**, 2353. (b) Tatsuma, T.; Matsui, H.; Shouji, E.; Oyama, N. *J. Phys. Chem.* **1996**, *100*, 14016. (c) Oyama, N.; Tatsuma, T.; Sato, T.; Sotomura, T. *Nature (London)* **1995**, *373*, 598. (d) Baron, M.; Wilson, C. V. *J. Org. Chem.* **1958**, *23*, 1021.
- (16) Hipler, F.; Girol, S. G.; Azzam, W.; Fischer, R. A.; Wöll, C. *Langmuir* **2003**, *19*, 6072.
- (17) (a) Garner, M.; Reglinski, J.; Cassidy, I.; Spicer, M. D.; Kennedy, A. R. *J. Chem. Soc., Chem. Commun.* **1996**, 1975. (b) Kimblin, C.; Hascall, T.; Parkin, G. *Inorg. Chem.* **1997**, *36*, 5680. (c) Reglinski, J.; Garner, M.; Cassidy, I. D.; Slavin, P. A.; Spicer, M. D.; Armstrong, D. R. *J. Chem. Soc., Dalton Trans.* **1999**, 2119. (d) Slavin, P. A.; Reglinski, J.; Spicer, M. D.; Kennedy, A. R. *J. Chem. Soc., Dalton Trans.* **2000**, 239. (e) Kimblin, C.; Bridgewater, B. M.; Hascall, T.; Parkin, G. *J. Chem. Soc., Dalton Trans.* **2000**, 891. (f) Dodds, C. A.; Lehmann, M.-A.; Ojo, J. F.; Reglinski, J.; Spicer, M. D. *Inorg. Chem.* **2004**, *43*, 4927.

and Marchio's thioxotriazolylborates.<sup>18</sup> We refer to this ligand and its derivatives as Janus scorpionates, after the Roman mythological god of gates and doors that is commonly depicted as a two-faced figure.<sup>19</sup> It was anticipated that different binding modes of this new ligand system would be observed depending on the choice of metal and that the electroactive nature of these ligands would also afford the opportunity to study the impact, if any, of metal complexation on the oxidation of the ligands. In this initial contribution, we describe the preparation, solid-state structures, solution characterization, and electrospray mass spectral characterization of the alkali metal and the noncoordinating tetrabutylammonium salts of this fascinating new class of scorpionate.

## Experimental Section

$\text{KBH}_4$  and  $\text{NaBH}_4$  purchased from Aldrich and 2-mercapto-1,3,4-thiadiazole purchased from Alfa Aesar were used without purification. Midwest MicroLab, LLC, Indianapolis, Indiana, performed all elemental analyses. IR spectra were recorded on a Nicolet Magna-IR 560 spectrometer.  $^1\text{H}$  and  $^{13}\text{C}$  NMR spectra were recorded on a Varian 300 MHz spectrometer. Chemical shifts were referenced to solvent resonances at  $\delta_{\text{H}} = 2.50$  and  $\delta_{\text{C}} = 39.51$  for DMSO. Melting point determinations were made on samples contained in glass capillaries using an Electrothermal 9100 apparatus and are uncorrected. Electrochemical measurements were collected under a nitrogen atmosphere at a scan rate of 200 mV/s for samples as 0.1 mM  $\text{CH}_3\text{CN}$  solutions with 0.1 M  $\text{NBu}_4\text{PF}_6$  as the supporting electrolyte. A three-electrode cell composed of an Ag/AgCl electrode, a platinum working electrode, and a glassy carbon counter electrode was used for the voltammetric measurements. Mass spectrometric measurements recorded in ESI(+) or ESI(-) mode were obtained on a Micromass Q-ToF spectrometer. For the ESI(+) experiments formic acid (approximately 0.1% v/v) was added to the mobile phase ( $\text{CH}_3\text{CN}$ ).

**Syntheses.**  **$\text{Na}[\text{HB}(\text{mtda})_3]$  (1).** Under argon, a finely divided mixture of  $\text{NaBH}_4$  (0.350 g, 9.25 mmol) and 2-mercapto-1,3,4-thiadiazole (4.37 g, 37.0 mmol) was placed in a 100 mL round-bottom flask which was subsequently connected to a calibrated gas collection meter. The reaction bulb was heated by an external oil bath to 150 °C over the course of 2 h total (with magnetic stirring of the mixture); gas evolution commenced when the oil bath reached 90 °C, was vigorous when the oil bath reached 120 °C (being 3/4 complete after 20 min at this temperature), and was complete (27.8 mmol  $\text{H}_2$  was collected) after the oil bath reached 150 °C and was held at that temperature for an hour. After it was cooled to room temperature, the resulting solid was washed first with three 20 mL portions of THF and then with three 20 mL portions of  $\text{CH}_3\text{OH}$  to remove unreacted starting heterocycle. The insoluble solid was dried at 60 °C under vacuum for 3 h to leave 3.07 g (86%) of the desired compound as a hygroscopic, colorless powder. mp: 225 °C (dec to pale yellow solid). Anal. Calcd (found) for  $\text{C}_6\text{H}_4\text{BN}_6\text{NaS}_6$ : C, 18.65 (18.42); H, 1.04 (1.22); N, 21.75 (21.55). IR ( $\text{cm}^{-1}$ , KBr pellet):  $\nu_{\text{BH}}$  2506, 2491. IR ( $\text{cm}^{-1}$ ,  $\text{CH}_3\text{CN}$ ):  $\nu_{\text{BH}}$  2504.  $^1\text{H}$  NMR (DMSO- $d_6$ ):  $\delta_{\text{H}}$  8.56 (s, 3H, HC=N).  $^{13}\text{C}$  NMR (DMSO- $d_6$ ):  $\delta_{\text{C}}$  188.9 (C=S), 145.1 (C=N). ESI(-) MS (relative intensity)

[assignment]: 363 (100) [ $\text{HB}(\text{mtda})_3 = \text{L}$ ], 749 (9) [ $\text{NaL}_2$ ], 1135 (8) [ $\text{Na}_2\text{L}_3$ ], 1521 (0.6) [ $\text{Na}_3\text{L}_4$ ]. ESI(+) MS (relative intensity) [assignment]: 365 (100) [ $\text{H}_2\text{L}$ ]<sup>+</sup>, 387 (40) [ $\text{HNaL}$ ]<sup>+</sup>, 409 (53) [ $\text{Na}_2\text{L}$ ]<sup>+</sup>, 428 (25) [ $\text{HNa}(\text{CH}_3\text{CN})\text{L}$ ]<sup>+</sup>, 450 (90) [ $\text{Na}_2\text{L}(\text{CH}_3\text{CN})$ ]<sup>+</sup>, 491 (68) [ $\text{Na}_2(\text{CH}_3\text{CN})_2\text{L}$ ]<sup>+</sup>, 532 (52) [ $\text{Na}_2(\text{CH}_3\text{CN})_3\text{L}$ ]<sup>+</sup>, 729 (12) [ $\text{H}_3\text{L}_2$ ]<sup>+</sup>, 751 (34) [ $\text{H}_2\text{NaL}_2$ ]<sup>+</sup>, 773 (41) [ $\text{HNa}_2\text{L}_2$ ]<sup>+</sup>, 795 (57) [ $\text{Na}_3\text{L}_2$ ]<sup>+</sup>, 1115 (1) [ $\text{H}_3\text{NaL}_3$ ]<sup>+</sup>, 1137 (4) [ $\text{H}_2\text{Na}_2\text{L}_3$ ]<sup>+</sup>, 1159 (10) [ $\text{HNa}_3\text{L}_3$ ]<sup>+</sup>, 1181 (1) [ $\text{Na}_4\text{L}_3$ ]<sup>+</sup>, 1501 (1) [ $\text{H}_3\text{Na}_2\text{L}_4$ ]<sup>+</sup>, 1523 (3) [ $\text{H}_2\text{-Na}_3\text{L}_4$ ]<sup>+</sup>, 1545 (4) [ $\text{HNa}_4\text{L}_5$ ]<sup>+</sup>, 1567 (6) [ $\text{Na}_5\text{L}_4$ ]<sup>+</sup>, 1911 (1) [ $\text{H}_2\text{-Na}_4\text{L}_5$ ]<sup>+</sup>, 1932 (2) [ $\text{HNa}_5\text{L}_5$ ]<sup>+</sup>, 1954 (4) [ $\text{Na}_6\text{L}_5$ ]<sup>+</sup>. High Resolution (Hi-Res) ESI(+) MS Calcd (obsd) for  $\text{C}_6\text{H}_4\text{BN}_6\text{Na}_2\text{S}_6$  [ $\text{Na}_2\text{L}^+$ ]: 408.8710 (408.8714). Hi-Res ESI(-) MS Calcd (obsd) for  $\text{C}_6\text{H}_4\text{-BN}_6\text{S}_6$  [ $\text{L}^-$ ]: 362.8915 (362.8905). Single crystals suitable for X-ray diffraction were grown by vapor diffusion of  $\text{Et}_2\text{O}$  into an acetone solution of the compound.

**$\text{K}[\text{HB}(\text{mtda})_3]$  (2).** A carefully ground mixture of  $\text{KBH}_4$  (0.550 g, 9.27 mmol) and 2-mercapto-1,3,4-thiadiazole (3.84 g, 32.5 mmol) was heated as described above. Hydrogen evolution began when the oil bath temperature reached 70 °C, was 3/4 complete when the bath reached 120 °C, and was complete within 2 h at 150 °C (27.8 mmol  $\text{H}_2$  was collected). After it was cooled to room temperature, the resulting solid was washed with three 20 mL portions of THF to remove unreacted 2-mercapto-1,3,4-thiadiazole. The resulting solid was dried by heating to 100 °C under vacuum for 2 h to give 2.24 g (60% based on  $\text{KBH}_4$ ) of pure  $\text{K}[\text{HB}(\text{mtda})_3]$  as a colorless powder. If the sample is not heated under vacuum, various amounts of THF remain coordinated depending on the time under vacuum, as determined by NMR and elemental analyses. mp: 238–239 °C. Anal. Calcd (found):  $\text{C}_6\text{H}_4\text{BKN}_6\text{S}_6$ : C, 17.91 (17.80); H, 1.00 (1.19); N, 20.88 (20.53). IR ( $\text{cm}^{-1}$ , KBr pellet):  $\nu_{\text{BH}}$  2501. IR ( $\text{cm}^{-1}$ ,  $\text{CH}_3\text{CN}$ ):  $\nu_{\text{BH}}$  2504.  $^1\text{H}$  NMR (DMSO- $d_6$ ):  $\delta_{\text{H}}$  8.56 (s, 3H, HC=N).  $^{13}\text{C}$  NMR (DMSO- $d_6$ ):  $\delta_{\text{C}}$  188.9 (C=S), 145.1 (HC=N). ESI(-) MS (relative intensity) [assignment]: 363 (100) [ $\text{HB}(\text{mtda})_3 = \text{L}$ ], 765 (3) [ $\text{KL}_2$ ], 1167 (1) [ $\text{K}_2\text{L}_3$ ], 1570 (0.01) [ $\text{K}_3\text{L}_4$ ]. ESI(+) MS (relative intensity) [assignment]: 365 (60) [ $\text{H}_2\text{L}$ ]<sup>+</sup>, 403 (71) [ $\text{HKL}$ ]<sup>+</sup>, 441 (100) [ $\text{K}_2\text{L}$ ]<sup>+</sup>, 485 (25) [ $\text{HK}(\text{CH}_3\text{-CN})_2\text{L}$ ], 729 (4) [ $\text{H}_3\text{L}_2$ ]<sup>+</sup>, 767 (34) [ $\text{H}_2\text{KL}_2$ ]<sup>+</sup>, 805 (58) [ $\text{HK}_2\text{L}_2$ ]<sup>+</sup>, 843 (60) [ $\text{K}_3\text{L}_2$ ]<sup>+</sup>, 1131 (1) [ $\text{H}_3\text{KL}_3$ ]<sup>+</sup>, 1169 (4) [ $\text{H}_2\text{K}_2\text{L}_3$ ]<sup>+</sup>, 1207 (6) [ $\text{HK}_3\text{L}_3$ ]<sup>+</sup>, 1245 (12) [ $\text{K}_4\text{L}_3$ ]<sup>+</sup>, 1534 (1) [ $\text{H}_3\text{K}_2\text{L}_4$ ]<sup>+</sup>, 1572 (2) [ $\text{H}_2\text{K}_3\text{L}_4$ ]<sup>+</sup>, 1610 (3) [ $\text{HK}_4\text{L}_5$ ]<sup>+</sup>, 1648 (5) [ $\text{K}_5\text{L}_4$ ]<sup>+</sup>, 1973 (0.5) [ $\text{H}_2\text{K}_4\text{L}_5$ ]<sup>+</sup>, 2011 (1) [ $\text{HK}_5\text{L}_5$ ]<sup>+</sup>, 2049 (2) [ $\text{K}_6\text{L}_5$ ]<sup>+</sup>. Hi-Res ESI(+) MS Calcd (obsd) for  $\text{C}_6\text{H}_4\text{BK}_2\text{N}_6\text{S}_6$  [ $\text{K}_2\text{L}^+$ ]: 440.8189 (440.8177). Single crystals of an acetonitrile solvate suitable for X-ray diffraction were obtained by vapor diffusion of  $\text{Et}_2\text{O}$  (over 4 days) into an acetonitrile solution of the compound.

**$\text{KNa}[\text{HB}(\text{mtda})_3]_2$  (3).** A mixture of 0.386 g (1.00 mmol)  $\text{Na}[\text{HB}(\text{mtda})_3]$  and 0.402 g (1.00 mmol)  $\text{K}[\text{HB}(\text{mtda})_3]$  was heated at reflux in 50 mL of  $\text{CH}_3\text{CN}$ , and 7 mL of DMF was added to effect dissolution. The resulting solution was filtered hot, cooled to room temperature, and layered with 250 mL of  $\text{Et}_2\text{O}$ . After the solvents were allowed to slowly diffuse over 2 days, the crystals were isolated by filtration and were dried to leave 0.775 g (98%) of **3** as a colorless powder. mp: 248–250 °C (dec to yellow solid). IR ( $\text{cm}^{-1}$ , KBr or  $\text{CH}_3\text{CN}$ ):  $\nu_{\text{B-H}}$  2504. Anal. Calcd (found) for  $\text{C}_{12}\text{H}_8\text{N}_{12}\text{S}_{12}\text{B}_2\text{NaK}$ : C, 18.15 (18.75); H, 1.02 (1.23); N, 21.17 (20.61).  $^1\text{H}$  NMR (DMSO- $d_6$ ):  $\delta_{\text{H}}$  8.56 (s, 6H, HC=N).  $^{13}\text{C}$  NMR (DMSO- $d_6$ ):  $\delta_{\text{C}}$  188.9 (C=S), 145.1 (HC=N). ESI(-) MS (relative intensity) [assignment]: 363 (100) [ $\text{HB}(\text{mtda})_3 = \text{L}$ ]<sup>-</sup>, 749 (0.05) [ $\text{NaL}_2$ ], 765 (0.1) [ $\text{KL}_2$ ]. ESI(+) MS (relative intensity) [assignment]: 365 (81) [ $\text{H}_2\text{L}$ ]<sup>+</sup>, 387 (16) [ $\text{HNaL}$ ]<sup>+</sup>, 403 (58) [ $\text{HKL}$ ]<sup>+</sup>, 409 (65) [ $\text{Na}_2\text{L}$ ]<sup>+</sup>, 425 (64) [ $\text{NaKL}$ ], 441 (100) [ $\text{K}_2\text{L}$ ]<sup>+</sup>, 729 (21) [ $\text{H}_3\text{L}_2$ ]<sup>+</sup>, 751 (7) [ $\text{H}_2\text{NaL}_2$ ]<sup>+</sup>, 767 (25) [ $\text{H}_2\text{KL}_2$ ]<sup>+</sup>, 773 (7) [ $\text{HNa}_2\text{L}_2$ ]<sup>+</sup>, 789 (23) [ $\text{HNaKL}_2$ ]<sup>+</sup>, 795 (6) [ $\text{Na}_3\text{L}_2$ ]<sup>+</sup>, 805 (30) [ $\text{HK}_2\text{L}_2$ ]<sup>+</sup>, 811

(18) (a) Bailey, P. J.; Lanfranchi, M.; Marchiò, L.; Parsons, S. *Inorg. Chem.* **2001**, *40*, 5030. (b) Cammi, R.; Gennari, M.; Giannetto, M.; Lanfranchi, M.; Luciano Marchiò, L.; Mori, G.; Paiola, C.; Pellinghelli, M. A. *Inorg. Chem.* **2005**, *44*, 4333.

(19) Further details regarding the remarkable coordination capabilities of this ligand towards both main group and transition metal complexes will be forthcoming.

(22)  $[\text{Na}_2\text{KL}_2]^+$ , 827 (38)  $[\text{NaK}_2\text{L}_2]^+$ , 843 (34)  $[\text{K}_3\text{L}_2]^+$ , 1093 (5)  $[\text{H}_4\text{L}_3]^+$ , 1115 (6)  $[\text{H}_3\text{NaL}_3]^+$ , 1131 (4)  $[\text{H}_3\text{KL}_3]^+$ , 1137 (2)  $[\text{H}_2\text{Na}_2\text{L}_3]^+$ , 1153 (1)  $[\text{H}_2\text{NaKL}_3]^+$ , 1169 (1)  $[\text{H}_2\text{K}_2\text{L}_3]^+$ , 1175 (0.5)  $[\text{HNa}_2\text{KL}_3]^+$ , 1181 (0.1)  $[\text{Na}_4\text{L}_3]^+$ , 1191 (4)  $[\text{HNaK}_2\text{L}_3]^+$ , 1197 (2)  $[\text{Na}_3\text{KL}_3]^+$ , 1207 (2)  $[\text{HK}_3\text{L}_3]^+$ , 1213 (4)  $[\text{Na}_2\text{K}_2\text{L}_3]^+$ , 1229 (5)  $[\text{NaK}_3\text{L}_3]^+$ , 1245 (3)  $[\text{K}_4\text{L}_3]^+$ . Hi-Res ESI(+) MS Calcd (obsd) for  $\text{C}_6\text{H}_4\text{BKN}_6\text{NaS}_6$   $[\text{NaKL}^+]$ : 424.8450 (424.8443). Single crystals of solvate mixtures with unknown composition suitable for X-ray diffraction can be obtained by vapor diffusion of  $\text{Et}_2\text{O}$  into either an acetone solution, a  $\text{CH}_3\text{CN}$  solution, or a DMF solution of the complex. The best quality crystals submitted for single-crystal X-ray diffraction (vide infra) were grown from the first solvent combination ( $\text{Et}_2\text{O}$ /acetone) and used samples that possibly contained trace THF.

**[NBu<sub>4</sub>][HB(mt<sub>3</sub>da)] (4).** A biphasic mixture of 1.00 g (2.59 mmol) of  $\text{Na}[\text{HB}(\text{mtda})_3]$  in 50 mL of water and 1.00 g (3.10 mmol) of  $\text{NBu}_4\text{Br}$  in 50 mL of  $\text{CH}_2\text{Cl}_2$  was vigorously stirred with occasional shaking for 30 min, and then the phases were separated. The aqueous phase was washed with two 25 mL portions of  $\text{CH}_2\text{Cl}_2$ , and the phases were separated. The combined organics were washed with two 25 mL portions of  $\text{H}_2\text{O}$ , and the phases were separated. The solvent was removed from the organic phase by vacuum distillation. The resulting solid was dried at 60 °C under vacuum overnight to leave 1.34 g (86% based on Na) of  $[\text{NBu}_4][\text{HB}(\text{mtda})_3]$  as a colorless solid. mp: 219–221 °C. Anal. Calcd (found) for  $\text{C}_{22}\text{H}_{40}\text{BN}_7\text{S}_6$ : C, 43.62 (43.35); H, 6.66 (6.87); N, 16.18 (16.28). IR ( $\text{cm}^{-1}$ , Nujol):  $\nu_{\text{BH}}$  2517. IR ( $\text{cm}^{-1}$ ,  $\text{CH}_3\text{CN}$ ):  $\nu_{\text{BH}}$  2504.  $^1\text{H}$  NMR (DMSO- $d_6$ ):  $\delta_{\text{H}}$  8.56 (s, 3H, HC=N), 3.13 (m, t,  $J = 8$  Hz, 8H,  $\text{NCH}_2$ ), 1.55 (m, 8H,  $\text{CH}_2$ ), 1.27 (m, 8H,  $\text{CH}_2$ ), 0.93 (t,  $J = 8$  Hz, 12H,  $\text{CH}_3$ ).  $^{13}\text{C}$  NMR (DMSO- $d_6$ ):  $\delta_{\text{C}}$  188.9 (C=S), 145.1 (C=N), 57.5, 23.1, 19.2, 13.5. ESI(–) MS: 363 (100)  $[\text{HB}(\text{mtda})_3 = \text{L}]$ , 968 (33)  $[(\text{NBu}_4)\text{L}_2]$ . ESI(+) MS: 242 (100)  $[\text{NBu}_4]^+$ , 365 (8)  $[\text{H}_2\text{L}]^+$ , 847 (1)  $[(\text{NBu}_4)_2\text{L}]^+$ . Hi-Res ESI(+) MS Calcd (obsd) for  $\text{C}_{38}\text{H}_{76}\text{BN}_8\text{S}_6$   $[(\text{NBu}_4)_2\text{L}^+]$ : 847.4610 (847.4626). Hi-Res ESI(–) MS Calcd (obsd) for  $\text{C}_{28}\text{H}_{44}\text{B}_2\text{N}_{13}\text{S}_{12}$   $[(\text{NBu}_4)_2\text{L}_2^-]$ : 968.0677 (968.0717). Single crystals of marginal quality for X-ray diffraction were grown by vapor diffusion of  $\text{Et}_2\text{O}$  into an acetone solution of the compound.

**Crystallography.** Crystals of **1** formed as long delicate fibers, the maximum thickness of which was <0.05 mm. X-ray intensity data from such a needle of **1**, a colorless bar of **2**· $\text{CH}_3\text{CN}$ , and a colorless needle of **3**·solvate were measured at 150(1) K on a Bruker SMART APEX diffractometer (Mo  $\text{K}\alpha$  radiation,  $\lambda = 0.71073$  Å).<sup>20</sup> While there were no apparent problems with the data collection for **2**· $\text{CH}_3\text{CN}$ , the crystal of **1** scattered only weakly because of its morphology. Also, because of the small size and weak scattering power of the crystal of **3**·solvate, no diffraction was observed above  $2\theta \approx 42^\circ$ , and the data for this derivative were truncated at this value. Raw data frame integration and Lp corrections for each data set were performed with SAINT+. Final unit cell parameters were determined by least-squares refinement of 2229 reflections from the data set of **1**, 8049 reflections from the data set of **2**· $\text{CH}_3\text{CN}$ , and 928 reflections from the data set of **3**·solvate, each with  $I > 5\sigma(I)$ . Analysis of the data for each showed negligible crystal decay during collection. Direct methods structure solution, difference Fourier calculations, and full-matrix least-squares refinement against  $F^2$  were performed with SHELXTL.<sup>21</sup> Hydrogen atoms were placed in geometrically idealized positions and included as riding atoms.

Other pertinent details regarding structure solution and refinement for each compound follows.

Systematic absences in the intensity data of **1** indicated the space groups  $P6_3mc$ ,  $P6_3/mmc$ ,  $P31c$ ,  $P31c$ , and  $P62c$ . After several space trial refinements, a reasonable solution was obtained in  $P31c$ . Upon completion, the structure was checked for additional symmetry elements with ADDSYM in PLATON, which verified the space group choice.<sup>22</sup> There are two crystallographically independent polymeric chains in the asymmetric unit, associated with Na1 and Na2/Na3. Atoms Na1 and B1/H1 of the Na1 chain are located on a 3-fold axis, and only 1/3 of the attached B1 ligand is symmetry independent. Atoms Na2, B2/H2, Na3, and B3/H3 of the Na2/Na3 chain are also located on a threefold axis, and there is 1/3 each of two additional ligands (B2 and B3) bonded to these atoms. The crystal was refined as a combined general twin and inversion twin, as described.<sup>21</sup> The twin operator is a 2-fold rotation around the crystallographic [110] direction, coupled with inversion twinning in each 2-fold related domain. Only atoms Na2, Na3, and the sulfur atoms were refined anisotropically; all remaining non-hydrogen atoms, except boron, were refined isotropically. Displacement parameters for the B atoms were fixed. The refinement difficulties are likely to be caused by the combined effects of the weak diffraction and the twinning.

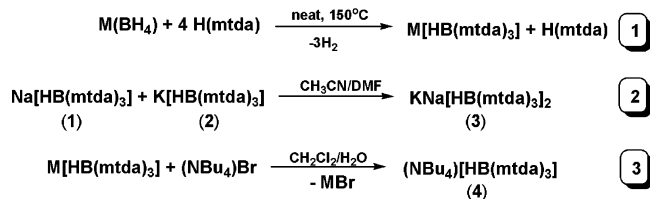
Compound **2**· $\text{CH}_3\text{CN}$  crystallizes in the orthorhombic system. Systematic absences in the intensity data were consistent with the space groups  $Pnma$  and  $Pna2_1$ ; intensity statistics indicated an acentric structure. The space group  $Pna2_1$  was eventually verified by successful solution and refinement of the data, manual examination of the structure, and ADDSYM/PLATON.<sup>22</sup> The asymmetric unit consists of one complete formula unit. All non-hydrogen atoms were refined with anisotropic displacement parameters. The final absolute structure (Flack) parameter was  $-0.03(4)$ , indicating the correct orientation of the polar axis and the absence of inversion twinning.

Compound **3** crystallizes as a solvate of undetermined composition in the trigonal crystal system. Systematic absences in the intensity data indicated the space groups  $P31c$  and  $P31c$ , the former of which was confirmed. The complex is located on a threefold axis of rotation passing through Na1, B1/H1, and near K1. B1/H1 and one  $\text{C}_2\text{HN}_2\text{S}_2$  ring are the only symmetry-independent part of the ligand. K1 is disordered about the threefold rotational axis. Refinement of K1 on the threefold axis yields a strongly oblate ellipsoid. Placement of K1 off the threefold axis gives a more reasonable ellipsoid and a refined site occupancy near 1/3, at which value the K1 occupancy was fixed for further cycles. The infinite tubular structure runs along the  $c$  axis at  $(1/3, 2/3, z)$  and  $(2/3, 1/3, z)$ . Between the tubes are channel-shaped voids along  $(0, 0, z)$  filled with disordered solvent. No reasonable solvent model could be obtained for the potential solvent species THF, acetone, and  $\text{Et}_2\text{O}$ . A second sample crystallized using a  $\text{CH}_3\text{CN}/\text{DMF}/\text{Et}_2\text{O}$  solvent system presented similar difficulties. Refinement of the first sample with the solvent peaks modeled as variable occupancy oxygen atoms showed the concentration of solvent is highest at  $z = 1/4$  and  $3/4$ . Although this treatment resulted in a reasonable refinement ( $R1 = 0.041$ , flat difference map), for final refinement, the contribution of these unknown solvent species were removed from structure factors with SQUEEZE ( $321.1 \text{ \AA}^3$  solvent-accessible void volume, 19% total unit cell volume,  $76 e^-/\text{cell}$ ).<sup>22</sup> The final tabulated FW,  $F(000)$ , and  $d_{\text{calcd}}$  represent known unit cell contents only. All non-hydrogen atoms were refined with anisotropic

(20) SMART, version 5.625, SAINT+, version 6.22, and SADABS, version 2.05; Bruker Analytical X-ray Systems, Inc.: Madison, WI, 2001.

(21) Sheldrick, G. M. SHELXTL, version 6.1; Bruker Analytical X-ray Systems, Inc.: Madison, WI, 2000.

(22) Spek, A. L. PLATON, A Multipurpose Crystallographic Tool; Utrecht University: Utrecht, The Netherlands, 2003.

**Scheme 1.** Preparation of Scorpionates Used in This Work<sup>a</sup><sup>a</sup> M = Na, K; mtda = 2-mercapto-1,3,4-thiadiazolyl.

displacement parameters. H2 was placed in the geometrically idealized position and included as an isotropic riding atom; H1 was located and refined freely.

**Results and Discussion**

**Synthesis.** The new alkali metal scorpionates are best prepared by heating an excess (more than three equivalents, with four or more being optimal) of the desired heterocycle with the appropriate alkali metal borohydride to between 150 and 190 °C, according to Scheme 1. In this way, 3 equiv of hydrogen (based on borohydride) are obtained, and the resulting product mixture contains the trisubstituted derivative and the remainder of the starting heterocycle. Unlike the related unsubstituted or 3-substituted poly(pyrazolyl)borate derivatives, using an even larger excess of heterocycle (5–7 equiv) does not produce tetrasubstituted compounds. Also, reaction mixtures containing excess heterocycle decompose regardless of cation giving unidentified intractable dark green solids when heated to 205 °C or more, rather than generating any well-defined tetrasubstituted borate derivatives. When the reactions are performed using exactly three equivalents of 2-mercapto-1,3,4-thiadiazole instead of an excess, the expected amount of hydrogen is obtained, but the product is typically a mixture of  $[\text{HB}(\text{mtda})_3^-]$ ,  $[\text{H}_2\text{B}(\text{mtda})_2^-]$ , and  $[\text{H}_3\text{B}(\text{mtda})^-]$ , along with free  $\text{H}(\text{mtda})$  ligand, as determined by NMR spectroscopy and independent syntheses of the components (vide infra).<sup>23</sup> Generally it is difficult to separate  $[\text{HB}(\text{mtda})_3^-]$  from  $[\text{H}_2\text{B}(\text{mtda})_2^-]$ , and the use of excess heterocycle minimizes the amount of the disubstituted borate. The desired sodium compound  $\text{Na}[\text{HB}(\text{mtda})_3]$  (1), however, can be separated from the product mixtures since it is far less soluble in  $\text{CH}_3\text{CN}$  (0.3 g/L) or  $\text{MeOH}$  (0.5 g/L) than the remaining components. As may be expected from the general trend that larger main group metal cations can achieve higher coordination numbers than their smaller congeners (through solvation), the compound  $\text{K}[\text{HB}(\text{mtda})_3]$  (2) is at least twice as soluble as its sodium counterpart in  $\text{CH}_3\text{CN}$  or  $\text{MeOH}$  (2 and 1 g/L respectively), and the corresponding difficulties in separation from the product mixtures lead to lower overall yields of pure potassium salt compared to the sodium derivative. The alkali metal salts are hygroscopic and are otherwise Lewis acidic, retaining most Lewis bases after exposure. However, the Lewis bases can generally be removed after prolonged heating under vacuum to give the pure “solvent-free” salts. The solvent-free salts are soluble in  $\text{H}_2\text{O}$ ,  $\text{DMSO}$ , and  $\text{DMF}$  and only slightly soluble in  $\text{MeOH}$ ,  $\text{CH}_3\text{CN}$ , acetone, and  $\text{THF}$ , but they are insoluble in  $\text{Et}_2\text{O}$ ,  $\text{CHCl}_3$ ,  $\text{CH}_2\text{Cl}_2$ , and hydrocarbons.

The mixed potassium–sodium salt  $\text{KNa}[\text{HB}(\text{mtda})_3]_2$  (3) was prepared with the intent to demonstrate the directed organization of heterobimetallic coordination polymers by the differential hard–soft coordination preferences of the metal ions and the bipolar coordination capabilities of the ligand. Thus, the mixing of ( $\text{CH}_3\text{CN}/\text{DMF}$ ) solutions of equimolar quantities of desired compounds (Scheme 1, middle), followed by solvent removal and crystallization, afforded the heterobimetallic product in a quantitative yield. It is important to note that  $\text{KNa}[\text{HB}(\text{mtda})_3]_2$  can also be isolated in trace quantity from the preparation of  $\text{K}[\text{HB}(\text{mtda})_3]$  because of a small but significant sodium impurity in commercially available  $\text{KBH}_4$  (98% purity). Finally, a derivative with a noncoordinating tetra(*n*-butyl)ammonium cation was prepared for the purpose of determining the impact, if any, of possible solution aggregation on the properties of the scorpionates. Thus, the ion exchange reaction between  $\text{Na}[\text{HB}(\text{mtda})_3]$  and  $(\text{NBu}_4)\text{Br}$  (Scheme 1, bottom) afforded the tetraalkylammonium derivative,  $(\text{NBu}_4)[\text{HB}(\text{mtda})_3]$  (4), in good yield. In contrast to its alkali metal counterparts, the alkylammonium salt is freely soluble in a variety of organic solvents such as  $\text{CHCl}_3$ ,  $\text{CH}_2\text{Cl}_2$ ,  $\text{THF}$ ,  $\text{CH}_3\text{CN}$ ,  $\text{CH}_3\text{OH}$ ,  $\text{DMF}$ , and  $\text{DMSO}$ ; a property that has proven beneficial for further synthetic procedures.

**Solid-State Structures.** The structures of 1–3 are given in Figures 2–4 respectively. Important bond distances and angles are summarized in Table 2. Numerous attempts were made to crystallize 4, but in the best case scenarios, such efforts produced rather poor quality crystals which resulted in highly disordered structures of marginal precision, only allowing general features of connectivity of the isolated ions to be established (Supporting Information). In the three alkali metal cases, polymer chains are formed by metal coordination to both the hard ( $\text{N}_3$ ) and soft ( $\text{S}_3$ ) portions of the bridging ligands, in stark contrast to the thioxotriazolylborate cousins which form discrete alkali metal complexes.<sup>18</sup> The B–H bond of the polymeric Janus scorpionates is always directed toward thione sulfurs rather than toward the nitrogen portion of the ligand. The sodium compound is remarkable in that there are, unexpectedly, two types of polymeric chains in the same crystal (Figure 2, top right and middle right) that can be differentiated on the basis of the line symmetry of the polymer chain dictated by the relative orientations of the B–H bonds along the lattice. In one chain, the B–H bonds are all oriented in the same direction resulting in a polar chain with simple *P1* (translational) line symmetry. The coordination environment about  $\text{Na}(1)$  in this chain is remarkable because there is a very short B–H··· $\text{Na}(1)$  interaction (such interactions typically average 2.51 Å)<sup>24,25</sup> of 2.33 Å ( $\text{Na}\cdots\text{B}$  3.26 Å) such that the metal center can best be described as seven-coordinate with the relatively rare capped-octahedral geometry. The average  $\text{Na}(1)$ –N (2.48 Å) and  $\text{Na}(1)$ –S (2.93 Å) distances, like the B–H··· $\text{Na}$  interactions, are relatively short but are in typical ranges ( $\text{Na}$ –N = 2.33–3.13 Å,  $\text{Na}$ –S = 2.82–3.19 Å) found for seven-coordinate sodium.<sup>24</sup>

(23) Full details results of these studies will be published separately.

(24) By comparison of the results of a Cambridge Structural Database search, see Supporting Information for full details.

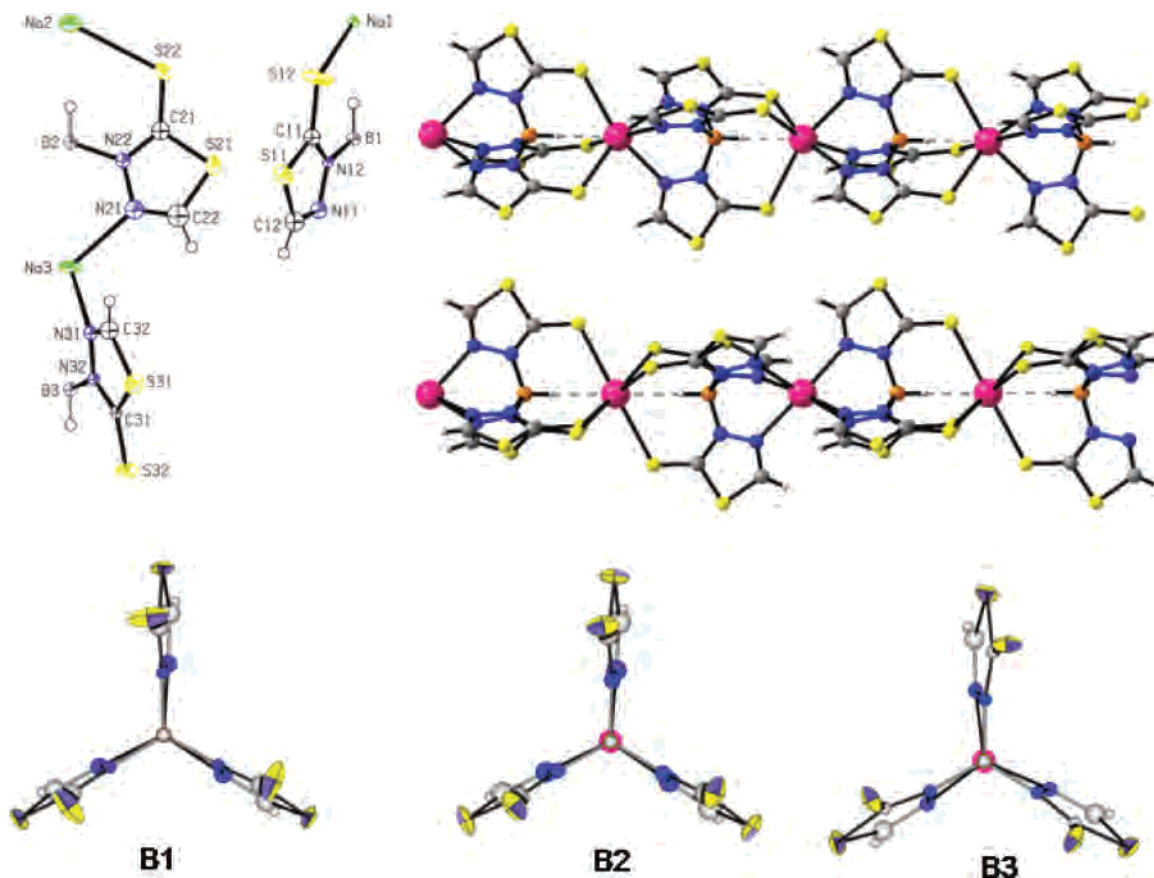


**Figure 2.** Solid-state structure of  $\text{Na}[\text{HB}(\text{mt-da})_3]$ , **1**: (top left) asymmetric unit, (top right) polar coordination polymer composed of  $\text{Na}(1)$ , (middle right) centric coordination polymer containing  $\text{Na}(2)$  and  $\text{Na}(3)$ , and (bottom row) view down pseudo- $C_3$  axes of scorpionate ligands bound to  $\text{Na}(1)$ ,  $\text{Na}(2)$ , and  $\text{Na}(3)$ , left to right, respectively.

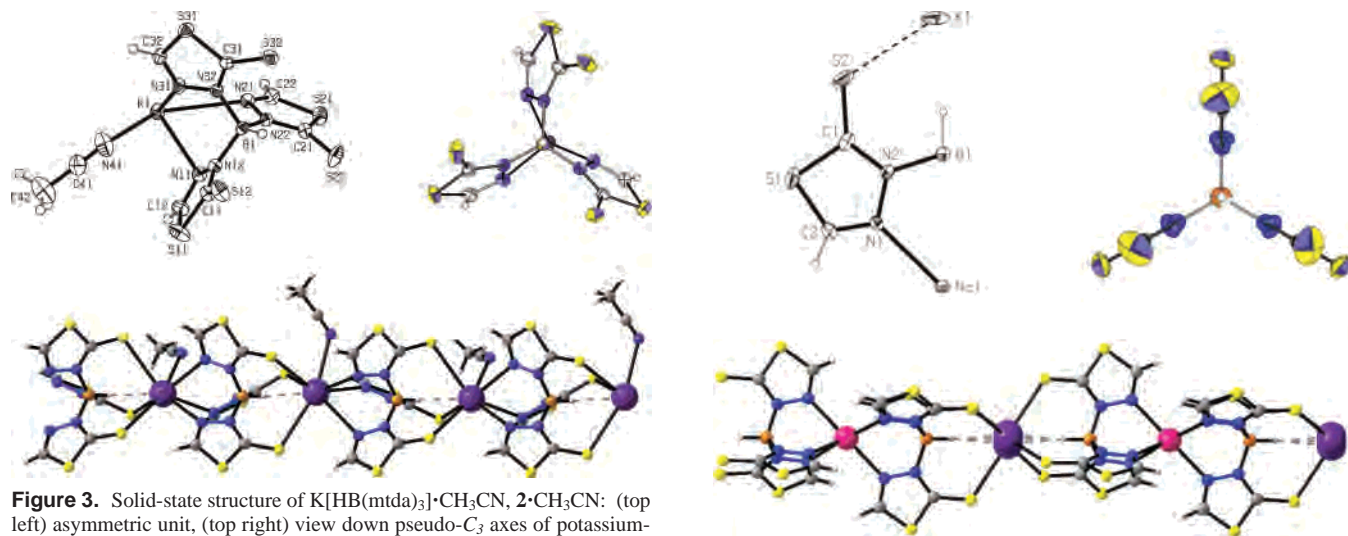


**Figure 3.** Solid-state structure of  $\text{K}[\text{HB}(\text{mt-da})_3] \cdot \text{CH}_3\text{CN}$ , **2**· $\text{CH}_3\text{CN}$ : (top left) asymmetric unit, (top right) view down pseudo- $C_3$  axes of potassium-bound scorpionate ligand, and (bottom) acentric coordination polymer propagating orthogonal to a  $2_1$  screw axis.

In the second type of coordination polymer in the lattice (Figure 2, middle right), the B–H bonds are alternately aligned (BH–HB BH–HB, etc.), resulting in a chain whose 1D representation would have approximate  $P2$  line symmetry with the  $C_2$  rotation axes located at the metal centers of the  $\text{Na}(2)\text{S}_6\text{H}_2$  and  $\text{Na}(3)\text{N}_6$  kernels. This chain deviates slightly from ideal  $P2$  line symmetry since the sodium centers are not truly situated at the centers of their respective coordination polyhedra. That is, for  $\text{Na}(2)$ , the metal resides closer

**Figure 4.** Solid-state structure of  $\text{KNa}[\text{HB}(\text{mt-da})_3]_2$ , **3**: (top left) asymmetric unit, (top right) view down the  $C_3$  axis, and (bottom) centric coordination polymer organized about alternating  $\text{Na}$  (pink) and  $\text{K}$  (purple) centers.

to the sulfur atoms bound to the scorpionate containing  $\text{B}(2)$  than to those sulfurs on the other scorpionate to which it is bound (containing  $\text{B}(3)$ ). Conversely,  $\text{Na}(3)$  is situated closer to the nitrogen atoms of the scorpionate containing  $\text{B}(3)$  than to those nitrogens of the scorpionate containing  $\text{B}(2)$ . Overall, there is a reciprocal relationship with these distortions (this and other distortions will be described in more detail in a

**Table 1.** Crystallographic Data Collection and Refinement for Na[HB(mtda)<sub>3</sub>] (**1**), K[HB(mtda)<sub>3</sub>]·CH<sub>3</sub>CN (**2**·CH<sub>3</sub>CN), and KNa[HB(mtda)<sub>3</sub>]<sub>2</sub>·solvate, (**3**·solvate)<sup>a</sup>

	<b>1</b>	<b>2</b> ·CH <sub>3</sub> CN	<b>3</b> ·solvate <sup>a</sup>
formula	C <sub>6</sub> H <sub>4</sub> BN <sub>6</sub> NaS <sub>6</sub>	C <sub>8</sub> H <sub>7</sub> BKN <sub>7</sub> S <sub>6</sub>	C <sub>12</sub> H <sub>8</sub> B <sub>2</sub> KN <sub>12</sub> NaS <sub>12</sub>
fw	386.31	443.48	788.73
cryst syst	trigonal	orthorhombic	trigonal
space group	<i>P</i> 31 <i>c</i>	<i>Pna</i> 2 <sub>1</sub>	<i>P</i> 31 <i>c</i>
<i>a</i> (Å)	13.6500(6)	15.0309(8)	11.7151(15)
<i>b</i> (Å)	13.6500(6)	13.7979(8)	11.7151(15)
<i>c</i> (Å)	13.6565(11)	8.6280(5)	14.239(3)
α (deg)	90	90	90
β (deg)	90	90	90
γ (deg)	120	90	120
<i>V</i> (Å <sup>3</sup> )	2203.6(2)	1789.40(17)	1692.5(4)
<i>Z</i>	6	4	2
<i>T</i> (K)	150(1)	150(1)	150(1)
ρ <sub>calcd</sub> (Mg m <sup>-3</sup> )	1.747	1.646	1.548
λ (Å)	0.71073	0.71073	0.71073
μ(Mo Kα) (mm <sup>-1</sup> )	0.954	1.002	0.938
R1 [ <i>I</i> > 2σ( <i>I</i> )]	0.0479	0.0271	0.0343
(all data)	(0.0530)	(0.0281)	(0.0572)
wR2	0.0861	0.0674	0.0643
(all data)	(0.0880)	(0.0681)	(0.0693)

<sup>a</sup> Acetone/THF/Et<sub>2</sub>O with an undetermined ratio.

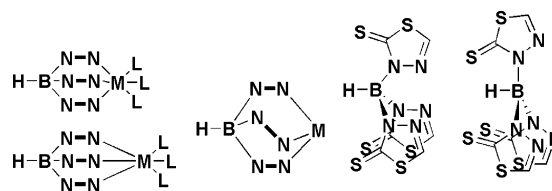
**Table 2.** Selected Average Bond Distances (Å) and Angles (deg) for Na[HB(mtda)<sub>3</sub>] (**1**), K[HB(mtda)<sub>3</sub>] (**2**·CH<sub>3</sub>CN), and KNa[HB(mtda)<sub>3</sub>]<sub>2</sub> (**3**)

	<b>1</b>			<b>2</b> ·CH <sub>3</sub> CN		<b>3</b>
	Na(1)	Na(2)	Na(3)	K(1)	K(1)	Na(1)
M–N <sup>a</sup>	2.475(7)		2.420(8) <sup>b</sup> 2.437(8) <sup>c</sup>	2.865(2)		2.426(3)
M–S	2.930(3)	2.910(4) <sup>b</sup> 2.960(4) <sup>c</sup>		3.310(1)	3.12 (3) <sup>d</sup>	
M–H	2.26	2.33 <sup>b</sup> 2.42 <sup>c</sup>		2.59	2.49(5) <sup>d</sup>	
M–Ct (N <sub>3</sub> )	1.73		1.62 <sup>b</sup> 1.68 <sup>c</sup>	2.21		1.68
M–Ct (S <sub>3</sub> )	1.31	1.34 <sup>b</sup> 1.38 <sup>c</sup>		1.83	1.62 <sup>d</sup>	
M···B	3.56	3.59	3.47 <sup>b</sup> 3.43 <sup>c</sup>	3.95	3.60 <sup>d</sup>	3.52
B–Ct (N <sub>3</sub> )	0.51		0.49 <sup>b</sup> 0.43 <sup>c</sup>	0.50		0.48
MN–NB	11.2		7.4 <sup>b</sup> 17.5 <sup>c</sup>	38.4		0.8

<sup>a</sup> Associated with scorpionate ligand. <sup>b</sup> For ligand with B(2). <sup>c</sup> For ligand with B(3). <sup>d</sup> Measured from centroid of potassium sites of disorder model.

later section) where the ligand with shorter M–S bonds has longer M–N bonds and vice versa. As with the polar Na(1) chain, short B–H···Na interactions of 2.33 and 2.42 Å (Na(2)–B(2) = 3.33 Å, Na(2)–B(3) = 3.42 Å) augment the coordination sphere of sulfur-bound sodium centers. In this case, such interactions render Na(2) eight-coordinate with a (distorted) bicapped octahedral geometry. The average Na–S distance in this chain of 2.935(4) Å is longer than in the previous chain, as expected, but it is the shortest yet reported for eight-coordinate sodium.<sup>24</sup>

The structures that contain potassium also include solvents of crystallization. In **2**, the solvent CH<sub>3</sub>CN is coordinated to the potassium, whereas in **3**, solvent fills channels in the structure. If one excluded the coordinated acetonitrile in **2**, a polar polymer chain with unidirectional B–H bonds is formed that resembles the chain with *P*1 line symmetry in the structure of **1**. In the current case, however, B–H···K agostic interactions, in addition to the coordinated CH<sub>3</sub>CN,



M–N bond-lengthening    ring twisting    boron pyramidalization

**Figure 5.** Common distortions in metal scorpionates where N–N represents a diazoyl ring such as a thiazadiazoyl or even a pyrazolyl.

renders the metal center eight-coordinate. The agostic interaction in **2**·CH<sub>3</sub>CN is quite short at 2.59 Å (B···K = 3.59 Å) compared to typical values for B–H···K agostic interactions which average 2.85 Å and range from 2.43 to 3.34 Å.<sup>24</sup> Moreover, the average K–S bond distance of 3.31 Å in **2**·CH<sub>3</sub>CN is shorter than 3.37 Å, the average distance found for all other eight-coordinate potassium compounds containing a potassium–sulfur bond.<sup>24</sup> Further, in 3D space, the polymer chain propagates along the *a* axis orthogonal to a 2<sub>1</sub> screw axis which is most evident by the alternating direction of the bound acetonitrile; when this effect is accounted for upon reduction to a one-dimensional (*P*1) line symmetry representation, a set of lattice points can be found at every other potassium center. The chain structure of **3**·solvate resembles that with *P*2 line symmetry of **1** but is organized with NaN<sub>6</sub> and KS<sub>6</sub>H<sub>2</sub> kernels, as might be expected from Pearson's hard–soft acid–base theory.<sup>14</sup> In this case, the potassium is disordered over three closely spaced positions in the lattice allowing the crystallographic 3-fold axis. The B–H···K agostic interaction of 2.49(5) Å (B···K = 3.61 Å) and average K–S bond distance of 3.13 Å, measured using the asymmetric unit, appear shorter than those found in **2** (Table 2); however, the disorder prohibits any meaningful comparisons.

The larger size (and higher coordination number) of the potassium cations compared to sodium induces significant distortions in the tripod ligand that impart important differences in the overall supramolecular structures and possibly the formation constants and thermodynamic stabilities of the resulting coordination polymers. A careful examination of these distortions is thereby important for the future design of potentially functional materials based on these and other one-dimensional hard–soft metalochains using this ligand system. As explained in more detail elsewhere,<sup>26</sup> there are three significant distortions (Figure 5) that allow semirigid tridentate scorpionate ligands to accommodate binding metals of varying sizes: M–N bond lengthening, heterocycle ring-twisting, and boron pyramidalization. The M–N bond lengthening distortion is easy to measure, and the effects are obvious. The larger average metal–nitrogen scorpionate bond distance of 2.865(2) Å in **2** versus the average Na–N distance of 2.475(8) Å in **1** partly contributes (the larger size of potassium versus sodium being more important) to the larger lattice constant of 7.525 Å versus 6.828 Å (ignoring CH<sub>3</sub>CN bonding in **2**) for the 1D chains of **2** and **1**, respectively (with idealized *P*1 line

(25) For instance, see: Reger, D. L.; Lindeman, J. A.; Lebioda, L. *Inorg. Chem.* **1988**, *27*, 1890 and references therein.

symmetry). For the specific case of the tris(mercaptothiadiazolyl)borates, which can bind metals via the soft sulfur donors, a related distortion, M–S bond lengthening, can also be identified. This distortion can be highlighted by the “NaS<sub>6</sub>” coordination environment around Na(2) in the centric chain of **1**. In this case, Na(2) actually sits closer to the three sulfurs of the borate ligand containing B(2) [Na(2)–Ct (S<sub>3</sub> of B2) = 1.34 Å] than the three sulfurs of the second capping scorpionate containing B(3) [Na(2)–Ct (S<sub>3</sub> of B3) = 1.38 Å]. Both of these distances are longer than the corresponding distance in the polar chain of **1** [Na(1)–Ct (S<sub>3</sub> of B1) = 1.31 Å], which might reflect the slightly different coordination environment about Na(1).

Two other distortions, ring-twisting and boron pyramidalization, require more sophisticated measurements, and their effects are more subtle than metal–ligand bond lengthening. Ring twisting is measured by the MN–NB torsion angle, and a metal-bonded scorpionate fragment with ideal C<sub>3v</sub> symmetry is expected to have a MN–NB torsion angle of 0°. For a given scorpionate with a generally fixed bite angle, the degree of twisting increases with the size of the metal. This effect is operative when the structures of the polar chains in **1** and **2** are compared. The smaller sodium derivative has less ring-twisting NaN–NB (11.2°) than KN–NB (38.4°) in **2**. A consequence of this ring twisting is a shortening of the M···B distance in the metallatrane framework. As an example, both centric chains in **1** and **3** share similar NaN<sub>6</sub> kernels with nearly identical average Na–N bond distances (2.44 Å for **1** and 2.43 Å for **3**), but the rings in **1** are more twisted (av NaN–NB of 17.5°) than in **3** (av NaN–NB of 0.8°), and consequently, the greater ring-twisting shortens the Na···B distance to 3.43 Å in **1** from 3.52 Å in **3**. Such a distortion may provide a mechanism to modulate the lattice spacings in future polymer chain systems based on this ligand. It should however be recognized that in the case of the polar chains in **1** and **3**, the difference in size between sodium and potassium cations likely dominates the increase in polymer chain lattice spacing of 13.66 Å for **1** to 14.24 Å for **3**, and any ring-twisting simply fine-tunes this spacing.

Finally, a distortion of significant importance to the formation and possibly the overall thermodynamic stability of the metallochains based on these new bipolar Janus scorpionates is the boron pyramidalization shown in the right of Figure 5. With this distortion, the B–N bond distances and B–N–N angles remain constant, but the N–B–N angles change. This distortion can be measured by the distance between boron and the centroid of the boron-bound nitrogens, B–Ct (N<sub>3</sub>). An ideal B–Ct (N<sub>3</sub>) distance of 0.52 Å can be estimated [(1.55 Å) cos(180 – 109.5°)] based on the average B–N distance of 1.55 Å found for all the known boron mercaptothiadiazolyl complexes, **1–4**, and using an ideal tetrahedral N–B–N bond angle. The B–Ct (N<sub>3</sub>) distances for the coordination polymers reported here are 0.51 (polar chain, **1**), 0.46 (av in nonpolar chain **1**), 0.50 (**2**), and 0.48 Å (**3**). As a matter of perspective, a related study has shown that the B–Ct (N<sub>3</sub>) distance varies between 0.48 and 0.62 Å for tris(pyrazolyl)borate complexes of iron(II) in high- and

low-spin states, where the effective sizes of the metal center in each spin state is strikingly different.<sup>25</sup> That is, the effectively larger metal center (high-spin Fe<sup>2+</sup>) had greater boron pyramidalization (shorter B–Ct (N<sub>3</sub>) distances), and the ligands were ultimately more distorted than those in the smaller low spin Fe<sup>2+</sup> form. In the case of the alkali metal tris(mercaptothiadiazolyl)borate complexes, large boron pyramidalization, in addition to the unfavorable energetics of the N–B–N bond angle strain, is anticipated to be especially unfavorable in heterobimetallic systems because it would encourage simultaneous binding of large metals to the hard nitrogen pocket and smaller metals to a small sulfur binding pocket. Conversely, a decrease of boron pyramidalization should relieve bond angle strain on boron and cause a concomitant decrease in the size of the nitrogen-binding pocket and increase in the size of the sulfur-binding pocket; a *synergistic* reciprocity that should bolster the hard–soft acid–base-directed self-assembly process. As a testament to the synergistic nature, the ligands in **3** are the least distorted of all those reported here which can be highlighted by comparing the ring-twisting and boron pyramidalization in **3** and the corresponding centric chain of **1** (Table 2); both parameters indicate that the larger potassium is a better fit than sodium for the MS<sub>6</sub>H<sub>2</sub> coordination pocket. Nevertheless, since the potassium center in **3** is in fact disordered over three closely spaced sites in the coordination pocket and because there is small but measurable ring-twisting (av MN–NB = 0.8°) in **3**, a cation other than potassium may prove to be even better compliment to sodium (or another metal other than sodium may be a better compliment to potassium) in a heterobimetallic polymer chain manifold; such a search is currently underway in our laboratories.

**Solution Properties.** The results of the solution studies indicate that the alkali metal Janus scorpionate complexes are dissociated in polar solvents, by the similarity in the NMR, IR, and electrochemical data of the alkali metal complexes **1–3** with those data for the tetrabutylammonium salt, **4**. For example, the NMR spectra of each derivative, **1–4**, in dimethylsulfoxide-*d*<sub>6</sub> are identical giving one resonance at δ<sub>H</sub> = 8.56 for the diazolyl ring hydrogen and two resonances at δ<sub>C</sub> = 188.9 and 145.1 for the thione and diazolyl ring carbons, respectively. The resonances for the hydrogen bound to the quadrupolar [*I*(<sup>11</sup>B) = 3/2] boron nucleus was not observed, as is typical in scorpionates. This same trend is maintained in other solvents as well (δ<sub>H</sub> = 8.46 for each in CD<sub>3</sub>OD and δ<sub>H</sub> = 8.25 for each in CD<sub>3</sub>CN), and this provides further evidence that the ligand is not coordinated to the alkali metals in solutions of **1–3**. If the alkali metals were coordinated to the ligand, the differences in electronegativities and solvation environments of the different metals in different solvents (and the gross change in the nature of the cation in **4**) should lead to detectable chemical shift changes in the resonances as delineated by the Ramsey equation.<sup>27</sup>

The IR spectral data also support the idea that the complexes are dissociated upon dissolution in polar solvents

(26) Reger, D. L.; Gardinier, J. R.; Elgin, J. D.; Smith, M. D.; Hautot, D.; Long, G. J.; Grandjean, F. *Inorg. Chem.* **2006**, *45*, 8862.



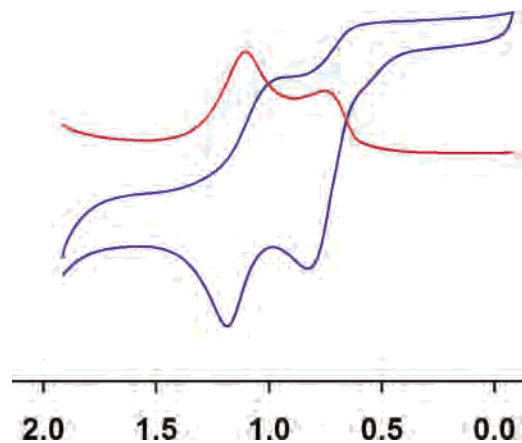


**Figure 6.** Cyclic and square-wave voltammograms for  $\text{K}[\text{HB}(\text{mtda})_3]$  (**3**) in acetonitrile (V vs Ag/AgCl). The voltammograms for the other compounds are identical.

such as  $\text{CH}_3\text{CN}$  or DMF. The B–H stretches in the solid-state (Nujol and KBr) IR spectra of compounds **1–4** depend on the counteranion. In the case of **1**, two overlapping weak intensity stretches are observed at  $2506$  and  $2491\text{ cm}^{-1}$ , in the typical region for B–H stretches. Nominally, these two bands can be attributed to the two different types of chains in the lattice. The other compounds show only one B–H stretch each:  $2501\text{ cm}^{-1}$  for **2**,  $2504\text{ cm}^{-1}$  for **3**, and  $2517\text{ cm}^{-1}$  for **4**. After the data for **4** were compared with those of the alkali metal compounds, **1–3**, the frequency of the B–H stretch of Janus scorpionates may prove to be a useful tool for quantifying the relative strength of the B–H $\cdots$ M interactions in the solid state, similar to the observations in metal poly(pyrazolyl)borate complexes.<sup>26</sup> That is, although the change is relatively small in the Janus scorpionates, the presence of B–H $\cdots$ M interactions serve to lower the B–H stretching frequency in a fashion similar to the way which the presence of hydrogen-bonding groups lower the stretching frequency of an O–H stretch, for example. Since the centric chain in **1** has, on average, longer B–H $\cdots$ Na interactions ( $2.38\text{ \AA}$ ) than the acentric chain ( $2.26\text{ \AA}$ ), we tentatively assign the band at  $2506\text{ cm}^{-1}$  to the B–H stretch of the centric chain and the band at  $2491\text{ cm}^{-1}$  to the B–H stretch of the acentric chain. Importantly, the solution IR spectra of **1–4** in  $\text{CH}_3\text{CN}$  are identical, showing one band of weak intensity for the B–H stretch at  $2504\text{ cm}^{-1}$ , indicating that the ligands are dissociated in solution.

The voltammograms of each compound in  $\text{CH}_3\text{CN}$  were also identical within experimental error and showed overlapping oxidation waves at  $+0.84$  and  $+1.07\text{ V}$  vs Ag/AgCl, whose shape was reminiscent of ECE-type behavior, as exemplified in Figure 6. We tentatively attribute this behavior to be caused by the oxidative formation of an electroactive disulfide linkage in the ligand, consistent with the known behavior of other thiadiazoline compounds.<sup>15</sup> Since there was no significant change in potential in the oxidation waves by changing counter-cations, it is highly likely that the metals are not coordinated to the ligand in  $\text{CH}_3\text{CN}$  solutions of **1–3**.

(27) Drago, R. S. *Physical Methods for Chemists*, 2nd ed.; Surfside Scientific Publishers: Gainseville FL, 1992; Chapter 7 and references therein.

Electrospray ionization mass spectral data are thought to accurately reflect the solution structure of species.<sup>7f,8d,8e,28</sup> While this line of thought may certainly be valid for kinetically inert complexes, caution should be exercised when interpreting ESI MS data from labile species, as exemplified by the seemingly puzzling data collected for the Janus scorpionates. All other characterization data (NMR, IR, and CV) suggested extensive dissociation in solution, yet in either positive or negative mode, many peaks for monoionic fragments of each **1–3** were observed, including those for polymetallic, polyligated fragments, that would be suggestive of the existence of coordination polymers. For instance, when operating under ESI(–) mode, the base peak observed for **1–4** was that at  $m/z = 363$  for the scorpionate ligand (L), and in the case of the alkali metal salts (M), the  $\text{ML}_2$ ,  $\text{M}_2\text{L}_3$ , and  $\text{M}_3\text{L}_4$  monoanionic fragments were also present. On the other hand, the ESI mass spectra of the mixed-metal system **3**, showed statistical mixtures of  $\text{Na}^+$  and  $\text{K}^+$  ions for each  $\text{M}_x\text{L}_y$  fragment, clearly indicative of ligand dissociation in solution. A similar observation was made for the mass spectrum of heterometallic **3** when operating under ESI(+) mode; the homometallic fragments  $[\text{HML}]^+$  (M = Na or K),  $[\text{Na}_2\text{L}]^+$ ,  $[\text{Na}_3\text{L}_2]^+$ ,  $[\text{K}_2\text{L}]^+$ , and  $[\text{K}_3\text{L}_2]^+$  are observed along with the mixed-metal species,  $[\text{KNaL}]^+$ ,  $[\text{K}_2\text{NaL}_2]^+$ , and  $[\text{Na}_2\text{KL}_2]^+$ , again clearly indicative of ligand dissociation. Thus, the ESI data support the remaining characterization that the ligands are dissociated in solution, but this point would have been missed if only homometallic coordination polymers were studied independently. Interestingly, the electrospray mass spectra of **4** reproducibly showed peaks for anionic  $[(\text{NBu}_4)(\text{L})_2]^-$  [ $m/z = 968$ , ESI(–)] and cationic  $[(\text{NBu}_4)_2\text{L}]^+$  [ $m/z = 847$ , ESI(+)] clusters, underscoring the importance of Coulombic interactions to ion pairing, even in the case where coordination polymers are not possible, although it is noteworthy that higher mass peaks, such as for  $(\text{NBu}_4)_2(\text{L})_3$  (or  $(\text{NBu}_4)_3\text{L}_2$  in the case of ESI(+) mode), were never detected.

## Conclusions

A new class of electroactive scorpionate ligands, the tris(mercaptothiadiazolyl)borates, has been developed that features characteristics of both the hard, tripodal nitrogen-donating tris(pyrazolyl)borates and the softer, tripodal sulfur-analogues, the tris(mercaptoimidazolyl)borates. These new scorpionates are designed to promote the controlled organization of metallochains according to Pearson's hard–soft acid–base theory.<sup>14</sup> An examination of structural data of **1–3** reveals that the size of the alkali metal cations dictates the extent of ligand distortions that occur upon metal binding, for homometallic systems the larger potassium cation produced larger ligand distortions than the corresponding

(28) For example, see: (a) Liu, C.-S.; Chen, P.-Q.; Yang, E.-C.; Tian, J.-L.; Bu, X.-H.; Li, Z.-M.; Sun, H.-W.; Lin, Z. *Inorg. Chem.* **2006**, *45*, 5812. (b) Reger, D. L.; Semeniuc, R. F.; Smith, M. D. *Eur. J. Inorg. Chem.* **2002**, 543. (c) Reger, D. L.; Semeniuc, R. F.; Smith, M. D. *Inorg. Chem. Commun.* **2002**, *5*, 278. (d) Yoshida, N.; Ichikawa, K.; Shiro, M. *Perkin Trans. 2* **2000**, *1*, 17. (e) Schalley, C. A.; Rivera, J. M.; Martin, T.; Santamaria, J.; Siuzdak, G.; Rebek, J., Jr. *Eur. J. Org. Chem.* **1999**, *6*, 1325.

sodium derivative. With the smaller sodium derivative, a unique structure with two different types of polymer chains was formed in the crystal lattice, an acentric chain with  $\text{NaN}_3\text{S}_3\text{H}$  kernels and a centric chain with alternating  $\text{NaN}_6$  and  $\text{NaS}_6$  kernels, suggesting that there is little energy difference between these two cases for this metal. In the potassium analogue, only a polar chain has been identified so far, possibly a result of the coordination preference of this larger cation for the softer sulfur (minimizing  $\text{KN}_6$  kernels). In the heterometallic K/Na system the larger potassium cation is bound to the sulfur portion of the ligand, while the smaller ion is bound to the nitrogen portion of the ligand, as anticipated from Pearson's hard-soft acid-base theory. Furthermore, the intrinsic ligand design may contribute thermodynamically to the self-assembly of heterometallic chains from the homometallic constituents. The binding of smaller cations to the hard donor likely relieves bond angle strain around boron and preorganizes the softer ligating sites at the opposite face of the ligand for binding to larger metals and vice versa. As testament to this preorganization, the ligands in the heterometallic coordination polymer chain were the least distorted of all those reported here. The large number of handles built into the ligand to probe the solution properties (NMR-active nuclei, B-H stretches for IR spectroscopy, and electrochemical activity)

provided evidence that the alkali metal salts of these uninegative scorpionate ligands are extensively dissociated or separately solvated and that the directed self-assembly process occurs during crystallization (and possibly during desolvation in the mass spectrometry experiments, further studies are underway to determine this latter hypothesis). We are currently pursuing other one-dimensional homo- and heterometallic polymer chain systems (main group and transition metal) using the Janus scorpionate to further delineate the factors that govern the self-assembly process and to identify whether the mercaptothiadiazolyl  $\pi$  systems can mediate electronic/magnetic interactions for future use as molecular wires.

**Acknowledgment.** We thank Professor Dan Reger for enlightening discussions and insightful comments. We thank Bill Cotham and Mike Walla (University of South Carolina) for obtaining the mass spectral data. J.R.G. thanks Marquette University and the Petroleum Research Fund for support.

**Supporting Information Available:** Figures of the structure of  $4 \cdot 0.5\text{CH}_2\text{Cl}_2$ , results of Cambridge Structural Database searches, and crystallographic information files (CIFs). This material is available free of charge via the Internet at <http://pubs.acs.org>.

IC0615877